coatings

MDPI

Article

Study on Deformation Force of Hard Aluminum Alloy Incremental Forming

Liang Wen [1], Yongjie Li [2], Silai Zheng [1], Hao Xu [2], Yunshuang Liu [1], Qiaolong Yuan [2], Yuanpeng Zhang [1], Hao Wu [2], Yuzhou Shen [2], Jizhou Kong [2] and Hongyu Wei [2,*]

[1] AVIC Chengdu Aircraft Industrial Co. Ltd., Chengdu 610092, China
[2] College of Mechanical and Electrical Engineering, Nanjing University of Aeronautics and Astronautics, Nanjing 210016, China
* Correspondence: whyme@nuaa.edu.cn

Abstract: The deformation force is an important factor affecting the forming accuracy of parts in the incremental forming process of sheet metal. This paper proposes an analytical calculation method of the deformation force based on pure shear deformation. After assuming and simplifying the factors affecting the deformation force, a graphical method is used to approximate the contact area between the forming tool and the sheet metal. A forming test is also designed. In addition, the deformation force is measured in the experiment, and its theoretical analysis value is compared with the actual measurement value of the forming test to validate the analytical method of deformation force calculation. The results show that the radial forming deviations are 28.5% and 22.5%, the axial deformation force deviations are 9.8% and 16.1%, and the forming force deviations are 6.3% and 10.3%, which demonstrates the effectiveness of using the analytical method to calculate the deformation force.

Keywords: incremental forming; deformation force; forming accuracy; pure shear deformation; measurement

Citation: Wen, L.; Li, Y.; Zheng, S.; Xu, H.; Liu, Y.; Yuan, Q.; Zhang, Y.; Wu, H.; Shen, Y.; Kong, J.; et al. Study on Deformation Force of Hard Aluminum Alloy Incremental Forming. *Coatings* **2023**, *13*, 571. https://doi.org/10.3390/coatings13030571

Academic Editor: Ben Beake

Received: 28 October 2022
Revised: 15 February 2023
Accepted: 17 February 2023
Published: 7 March 2023

1. Introduction

The traditional stamping and forming process typically requires relatively expensive punch and concave dies. In addition, the die manufacturing cycle is long and expensive, and it is therefore difficult to quickly change the new customer needs. This new market demand can be met using digital incremental forming [1–3], which is a new sheet metal flexible rapid prototyping technology [4–6]. In contrast to the traditional stamping forming, this technology can produce sheet metal parts with large forming limits and complex shapes without the use of a special die, or by simply using model support, which makes it ideal for rapid prototyping and small batch production [7–11].

The incremental forming process is complicated, and the lack of precision after forming is the main issue impeding the advancement of the process. Studying the forming force is the most direct entry point into the study of the incremental forming process mechanism. It is useful for predicting the forming accuracy in the incremental forming process, and it provides a theoretical foundation and guidance for the trial production of special forming equipment. Consequently, if the deformation force calculation method can be performed through deformation zone mechanics analysis, researchers can predict the forming accuracy in advance, and then modify the forming parameters to improve the precision of the part [12–14].

Many researchers calculate the forming force primarily from the mechanism and after analyzing the stress and strain in the plate's deformation area [15–17]. Some studies have used the finite element software to create a finite element model and simulate the forming force. Experiments have also been conducted in this field [18–21]. Using intelligent algorithms, empirical models were obtained, and forming forces for the incremental forming

processes were predicted [22,23]. Silva et al. [24] used the membrane analysis method to calculate the forming force when processing conical and square cones. The basic principle of their study is to ignore the thickness of the sheet and approximate its deformation with a plane strain state. Chang et al. [25,26] proposed the membrane analysis method [24]. Improvements have been made on this basis, and the forming force prediction models of the single-point incremental forming and multi-pass forming have been developed, which greatly improved the prediction accuracy. After observing the shape of the contact area between the plate and the tool head, Aerens et al. [27] developed an empirical model for predicting the forming force. Li et al. [28] and Aerens et al. [27] established the finite element model of the incremental forming process to analyze the forming mechanism of the incremental forming process. Li et al. [28] proposed an efficient forming force prediction analysis model based on the finite element model, which simultaneously considered the influence of bending, shearing, and stretching on the forming force when processing square cones.

Although many studies have been conducted on the forming force of the incremental forming process, these studies have some limitations. In this paper, it is assumed that the stress state of the contact deformation zone during the incremental forming process of sheet metal is the superposition of pure shear stress and hydrostatic pressure, and thus the deformation of the material is a pure shear deformation. The analytical calculation method of the deformation force is deduced after using the graphic method to approximate the contact area between the forming tool and the metal sheet, based on the pure shear deformation. This is performed after making assumptions and simplifications on the factors affecting the deformation force in the forming process. A set of forming tests is then designed, and the deformation force is measured using a Kistler 9443B three-way piezoelectric force measuring instrument. Finally, the theoretical deformation force analysis value is compared with the actual measurement value of the forming test in order to validate the normal deformation force calculations.

2. Analysis of the Sheet Metal Incremental Forming Process

2.1. The Principle of Incremental Forming

Incremental forming consists of introducing the rapid prototyping technology known as "layered manufacturing". In the incremental forming process (Figure 1), the sheet metal is fixed along the edge by a simple fixture, the forming tool is driven by a special NC device to press the sheet metal according to the pre-prepared NC program command, and the forming tool is then driven by the forming device to continuously move along the sheet metal surface according to the pre-prepared NC program. In the forming process, the forming tool locally contacts the sheet metal. A tiny area around the contact point is under high pressure due to its force, and local plastic deformation occurs. Thus, the continuous movement of the forming tool is accompanied by the continuous local plastic deformation of the sheet metal. The required part shape can be obtained by accumulating this continuous local plastic deformation [29].

2.2. Mechanical Analysis of the Deformation Zone

During the forming process, the forming tool starts to contact the metal sheet from point D and leaves the sheet at point C, and the sheet metal has contact deformation in the CD area, as shown in Figure 1. That is, under the action of the forming tool, the sheet metal has local contact plastic deformation, starting from point D and ending at point C. Therefore, the CD area can be considered as the deformation area in the forming process.

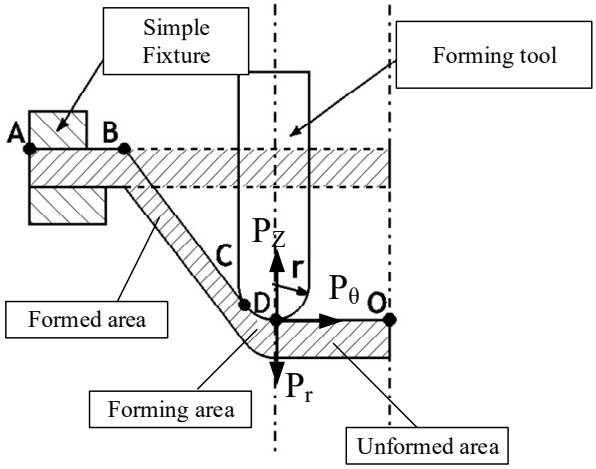

Figure 1. Progressive forming mechanism.

As a result of the local effect of the forming tool, the metal material in the deformation area undergoes plastic deformation under the action of radial and tangential tensile stresses. In other words, the material is in a state of two-way tensile stress, the billet is radially stretched, the thickness direction is thinner, and the tangential direction has not changed. Figure 2 shows the stress-strain relationship. The constitutive equation reveals the following relationships [30,31]:

$$\begin{cases} \varepsilon_r = \frac{\bar{\varepsilon}}{\bar{\sigma}}[\sigma_r - \frac{1}{2}(\sigma_t + \sigma_\theta)] \\ \varepsilon_t = \frac{\bar{\varepsilon}}{\bar{\sigma}}[\sigma_t - \frac{1}{2}(\sigma_r + \sigma_\theta)] \\ \varepsilon_\theta = \frac{\bar{\varepsilon}}{\bar{\sigma}}[\sigma_\theta - \frac{1}{2}(\sigma_r + \sigma_t)] \end{cases} \tag{1}$$

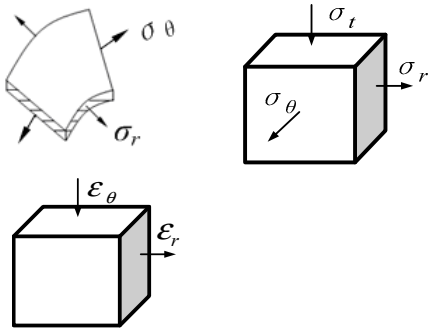

Figure 2. Stress-strain state of the contact deformation zone.

According to the yield criterion, there are:

$$\sigma_r - \sigma_t = \beta\sigma_s \tag{2}$$

According to the constant volume law, it is:

$$\varepsilon_r + \varepsilon_t + \varepsilon_\theta = 0 \tag{3}$$

As the stress value σ_t in the thickness direction is much smaller than σ_r and σ_θ during the contact deformation process, it can be approximated that it is null. In addition, during the forming process, there is no tangential deformation. That is, ε_θ is null. If $k = 1.1$ and $\sigma_s = \sigma_{sm}$ (the average deformation resistance of the studied instantaneous deformation area), Equations (1)–(3) can be simultaneously obtained:

$$\begin{cases} \sigma_r = 1.1\sigma_{sm} \\ \sigma_\theta = 0.55\sigma_{sm} \end{cases} \tag{4}$$

3. Calculation of the Deformation Force

The deformation force is a crucial parameter that affects the forming quality in the sheet metal incremental forming process. The amount of deformation force is one of the criteria for selecting the forming equipment. It is also one of the parameters used for controlling the forming accuracy. The calculation of the deformation force is difficult and it depends on several parameters [16].

3.1. Material Deformation Analysis

According to the above analysis, the stress state at any position on the contact deformation zone can be obtained:

$$\sigma_{ij} = \begin{bmatrix} 1.1\sigma_{sm} & 0 & 0 \\ 0 & 0.55\sigma_{sm} & 0 \\ 0 & 0 & 0 \end{bmatrix} \tag{5}$$

The stress tensors of Equation (5) are rewritten into the form of the stress deviator tensor and stress sphere tensor as:

$$\sigma_{ij} = \sigma'_{ij} + \delta_{ij}\sigma_m \tag{6}$$

where σ_{ij} is the stress deviator and σ_m is the Average stress

Therefore, the deviatoric stress tensor is expressed as:

$$\sigma'_{ij} = \begin{bmatrix} 0.55\sigma_{sm} & 0 & 0 \\ 0 & 0 & 0 \\ 0 & 0 & -0.55\sigma_{sm} \end{bmatrix} \tag{7}$$

The above analysis shows that, during the forming process, the contact denatured zone can be considered as a hydrostatic pressure superimposed by deviatoric stress. During forming, the hydrostatic pressure can only affect the volume of the metal sheet, and not its shape (plastic deformation). The deviatoric stress can only change the shape (plastic deformation) of the metal sheet, but it cannot change its volume. Therefore, the plastic deformation of the material is caused by the deviatoric stress. It can be seen from Equation (7) that the deformation of the contact zone meets the condition of plane pure shear deformation. That is, the principal stresses in two opposite directions have the same size, and those in the other direction are null. Consequently, the material deformation in the contact zone during sheet metal incremental forming can be classified as pure shear deformation.

3.2. Tangential Deformation Force

As the material deformation in the process of sheet metal incremental forming conforms to the condition of plane pure shear deformation, it can be assumed that the material has only shear deformation along the axis of the forming tool during the deformation process. That is, the incremental forming process is assumed to be an ideal deformation diagram (Figure 3), and the material slides along the axis to the inclined plane with the forming angle.

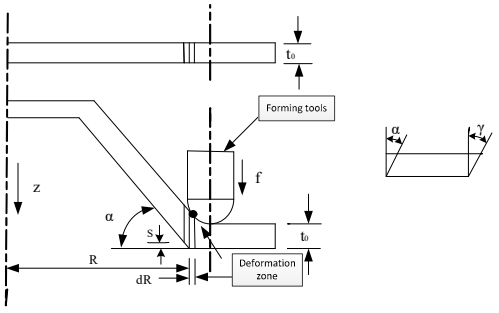

Figure 3. Schematic of the deformation.

According to this assumption, only the shear strain on the R_Z plane occurs in the deformed material. It can be seen from Figure 3 that R is the distance from the center of the blank to the axis of rotation, and s is the unit having a thickness of dR and sliding along the axis. Therefore, the shear strain is equal to the distance s of the axial slip of the element divided by its thickness dR:

$$\gamma = \frac{s}{dR} = \mathrm{tg}\alpha \tag{8}$$

where α is the forming angle.

The value of the tangential force P_θ can be derived according to the equilibrium condition of the work that is conducted and the deformation work. If the shear stress on the material is τ and the shear strain is γ, the plastic deformation work per unit volume of the material is expressed as:

$$w = \int_0^{\gamma} \tau \cdot d\gamma = \int_0^{tg\alpha} \tau \cdot d\gamma \tag{9}$$

Due to the deformation hardening of the material, τ will be a function of γ. In addition, because the τ-γ curve is more difficult to obtain than the σ-ε (-) stretching curve, Equation (9) can be rewritten as:

$$w = \int_0^{\bar{\varepsilon}} \sigma \cdot d\bar{\varepsilon} \tag{10}$$

where σ is the tensile stress of the material (N/mm).

According to the "deformation energy constant condition", the relationship between γ and ε shows that the actual equivalent effect in the incremental forming process becomes:

$$\bar{\varepsilon} = \frac{1}{\sqrt{3}}\gamma = \frac{1}{\sqrt{3}}\mathrm{tg}\alpha \tag{11}$$

Assuming that, during the forming process, the radius of the part at the forming position is R, the rotational speed of the forming tool is n, the feed of the tool along the axis of the workpiece is f, the initial thickness of the sheet is t_0, and the wall thickness of the part at the forming position is $t = t_0 \cos\alpha$, the volume change rate of the material per unit time in incremental forming is then given by:

$$\begin{array}{l} \frac{\mathrm{d}V}{\mathrm{d}T} = 2\pi n \cdot R \cdot t_0 \frac{dR}{dT} \\ = 2 \cdot \pi n \cdot R \cdot t_0 \cdot f \cdot \mathrm{ctg}\alpha \end{array} \tag{12}$$

Therefore, the machining power N, the corresponding torque M_t, and the tangential force P_θ can be computed as:

$$N = w \cdot \frac{dV}{dT} = 2\pi \cdot t_0 \cdot f \cdot n \cdot R \cdot \int_0^{\bar{\varepsilon}} \sigma d\bar{\varepsilon} \tag{13}$$

$$M_t = \frac{N}{2 \cdot \pi \cdot n} = t_0 \cdot f \cdot R\mathrm{ctg}\alpha \cdot \int_0^{\bar{\varepsilon}} \sigma d\bar{\varepsilon} \tag{14}$$

$$Pt = \frac{Mt}{R} = t0 \cdot f \cdot ctg\alpha \cdot \int_0^{\bar{\varepsilon}} \sigma d\bar{\varepsilon} \tag{15}$$

$$P_\theta = \frac{M_t}{R} = t_0 \cdot f \cdot ctg\alpha \cdot \int_0^{\bar{\varepsilon}} \sigma \cdot d\bar{\varepsilon} \tag{16}$$

When the forming process parameters are determined, the values of N, M_t, and P_t can be obtained. However, as σ is a function of ε, the average stress can be used to simplify the calculation:

$$\overline{\sigma 0} = (\int_0^{\varepsilon} \sigma d\varepsilon)/\bar{\varepsilon} \tag{17}$$

This can be approximated by the arithmetic mean of $\sigma_{0.2}$ and σ_n (the actual stress corresponding to the tensile actual stress-strain curve). By substituting Equation (11) into Equation (16), the tangential force P_θ can be calculated as:

$$P_\theta = t_0 \cdot f\mathrm{ctg}\alpha \cdot \overline{\sigma_0} \cdot \bar{\varepsilon} = \frac{1}{\sqrt{3}} \cdot t_0 \cdot f\mathrm{ctg}\alpha \cdot \overline{\sigma_0} \cdot \tan\alpha \tag{18}$$

3.3. Radial and Axial Deformation Forces

It is assumed that the average pressure p is the contact surface between the forming tool and the workpiece during the incremental forming process. The projected areas of the contact surface in the tangential, radial, and axial directions are F_θ, F_r, and F_z, respectively. The components of the force in the three directions are then given by:

$$\begin{cases} P_\theta = p \cdot F_\theta \\ P_r = p \cdot F_r \\ P_z = p \cdot F_z \end{cases} \tag{19}$$

Therefore, the radial forces P_r and P_z can be expressed as:

$$\begin{cases} P_r = P_t \frac{F_r}{F_\theta} \\ P_z = P_t \frac{F_z}{F_\theta} \end{cases} \tag{20}$$

The projected areas F_θ, F_r, and F_z in the three directions can be determined using the method of drawing and analysis.

The drawing method projects the contact area between the tool and the workpiece in three directions. It is challenging to accurately define these three projected figures' outlines by a formula. According to the results of the drawing, the following approximate calculations can be made:

$$\begin{cases} a \approx r_r \cdot \sin\alpha \\ b = R \cdot \theta \\ c = f \\ d \approx r_r (1 - \cos\alpha) \end{cases} \tag{21}$$

where r_r is the forming tool ball nose radius and θ is the angle of the deformation zone.

The included angle of the deformation zone is given by:

$$\theta = \frac{\pi}{180} \arccos\left[\frac{c - \sqrt{1 + \frac{b^2}{R^2} \cdot (c-1)}}{(c-1)} \right] \tag{22}$$

a, b, c, and d have the following relationship:

$$\begin{cases} a^2 = r_r^2 - r_1^2 \\ r_1 = r_r - f \\ b^2 = 2H \cdot a + a^2 \\ c = \frac{b^2}{a^2} \end{cases} \tag{23}$$

where H is the forming tool height.

The contour values of the three projection diagrams are then obtained, as shown in Figure 4. They are approximately processed according to the area of the triangle:

$$\begin{cases} F_\theta \approx \frac{1}{2} f \cdot r_r \cdot \sin\alpha \\ F_r \approx \frac{1}{2} f \cdot r_r \cdot (1 - \cos\alpha) \cdot R \cdot \theta \\ F_z \approx \frac{1}{2} r_r \cdot \sin\alpha \cdot R \cdot \theta \end{cases} \tag{24}$$

By substituting Equation (22) into Equation (20), the following can be obtained:

$$\begin{cases} P_r = P_\theta \cdot \frac{(1-\cos\alpha) \cdot R \cdot \theta}{f \cdot \sin\alpha} \\ P_z = P_\theta \cdot \frac{R \cdot \theta}{f} \end{cases} \tag{25}$$

The tangential, radial, and axial forming forces, as well as the forming force, can be obtained from the above analysis:

$$\begin{cases} P_\theta = \frac{1}{\sqrt{3}} t_0 \cdot f \cdot \overline{\sigma_0} \cdot \tan\alpha \\ P_r = P_\theta \cdot \frac{(1-\cos\alpha) \cdot R \cdot \theta}{f \cdot \sin\alpha} \\ P_z = P_\theta \cdot \frac{R \cdot \theta}{f} \\ P = \sqrt{P_\theta^2 + P_r^2 + P_z^2} \end{cases} \tag{26}$$

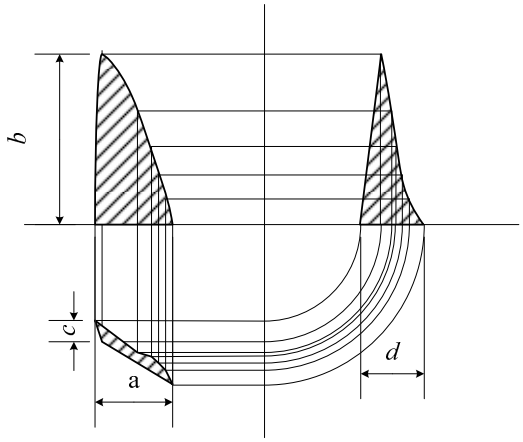

Figure 4. Projection of the forming tool and the plate contact area.

As P_θ << [P_r, P_z], the deformation force can be simplified as:

$$P = \sqrt{P_r^2 + P_z^2} \tag{27}$$

4. Materials and Methods

4.1. Experimental Materials

To verify the validity of the previous deformation force calculation formula, two conical parts, with forming angles of 45° and 58°, heights of 50 mm and 25 mm, and opening radii of 55.4 mm and 33.6 mm, are designed, as shown in Figures 5 and 6. The material of the designed punches is tool steel, and the diamond film is sputtered after quenching. The surface of the processed punch is intact and can meet the requirements of high-performance forming applications.

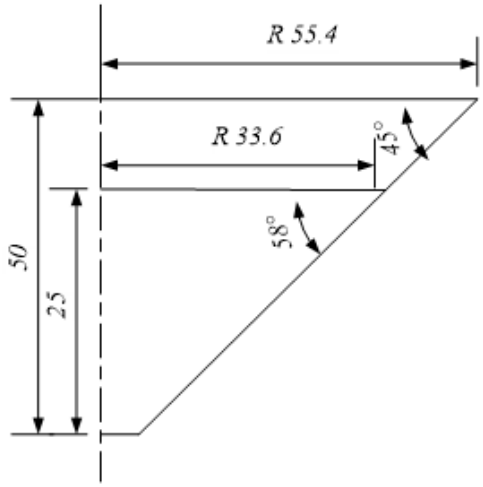

Figure 5. Theoretical models of the test parts and actual parts.

4.2. Experimental Method

In this study, a three-dimensional theoretical model of the test component was developed using the CAD/CAM software. Numerical control programming based on the model was then conducted, creating the processing path and outputting the processing instructions of the numerical control forming equipment. The forming test conditions are shown in Table 1.

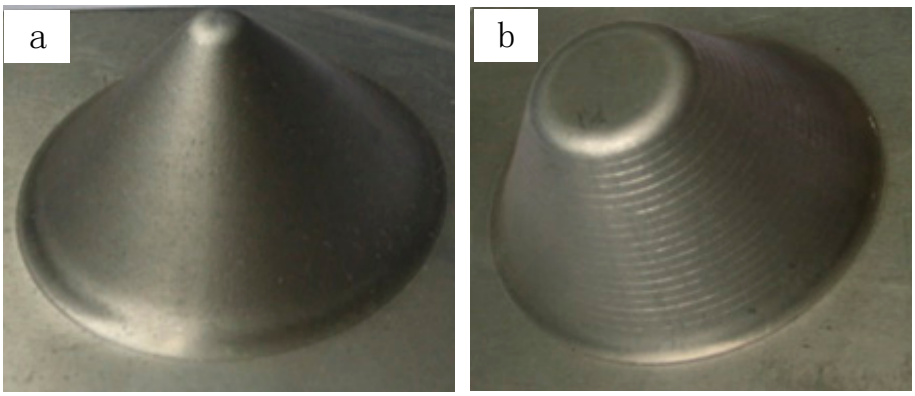

Figure 6. Experimental molded parts: (**a**) the specimen with forming angles of 45° and (**b**) the specimen with forming angles of 58°.

Table 1. Conditions of the forming experiment.

Project	Specimen 1	Specimen 2
Forming equipment	Incremental forming machine	Incremental forming machine
Forming tool diameter	Φ8 mm	Φ8 mm
Sheet material	LY12M	LY12M
Blank size	Φ80 mm	Φ130 mm
Blank thickness	1.4 mm	1.4 mm
Lubricating oil	L–ECC 30	L–ECC 30

4.3. Deformation Force Measurement Solution

The deformation force was measured using a Kistler 9443B three-way piezoelectric dynamometer. The fixture for securing the metal sheet was placed above the dynamometer (Figure 7), so that the forming tool operates on the metal plate during the forming process. The material's force will be completely transmitted to the dynamometer.

Figure 7. Measurement diagram of the deformation force.

5. Analysis of Experimental Results

5.1. Results of the Deformation Force Measurement

Deformation forces in three directions can be obtained by measuring using a Kistler 9443B three-way piezoelectric force gauge, as shown in Figures 8 and 9. The relationship between the deformation forces F_x,F_y, and the radial forming F_r at any position P on the forming plane is given by (Figure 10):

$$\begin{cases} F_x = F_r \cos(\varphi) \\ F_y = F_r \cos(\varphi + \pi/2) \end{cases} \quad (28)$$

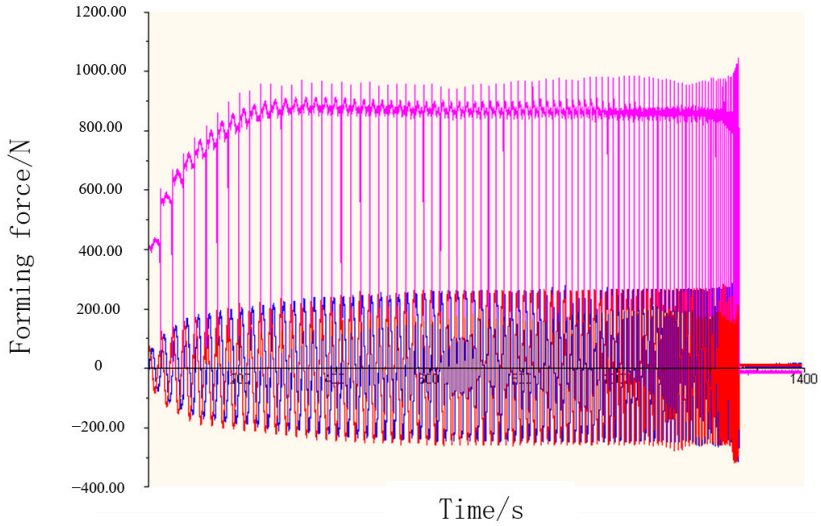

Figure 8. Deformation force measured by experiment 1.

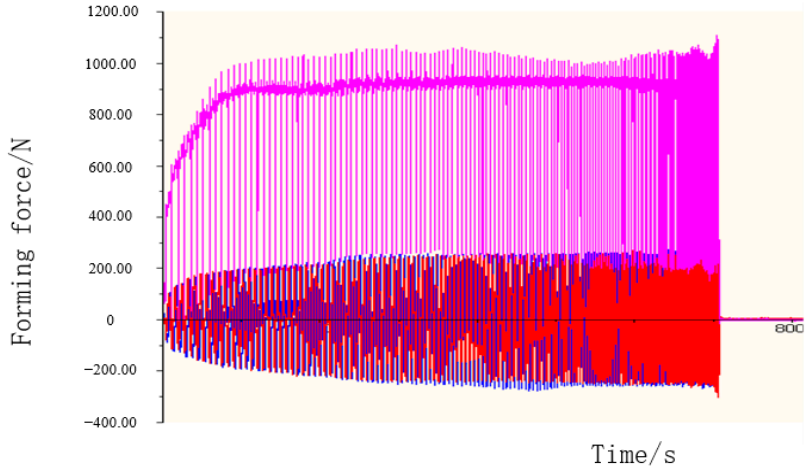

Figure 9. Deformation force measured by experiment 2.

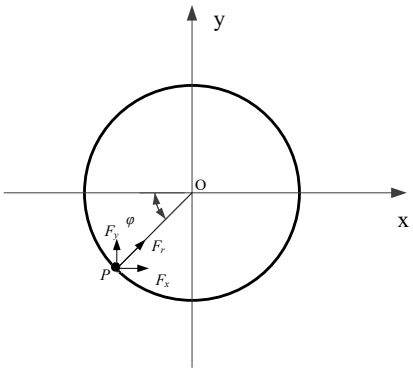

Figure 10. Schematic diagram of the deformation force relationship on the forming plane.

The deformation force in the *xy* direction is periodic. During the forming process, each contour layer can be considered as a cycle with two peaks. The two peaks have essentially the same size and opposite directions. The radial deformation force on the modified forming plane is defined as the average of the absolute value of the peak value, while the axial deformation force is defined as the average value of the z-direction force at any ten points on the contour layer, as shown in Figures 11 and 12.

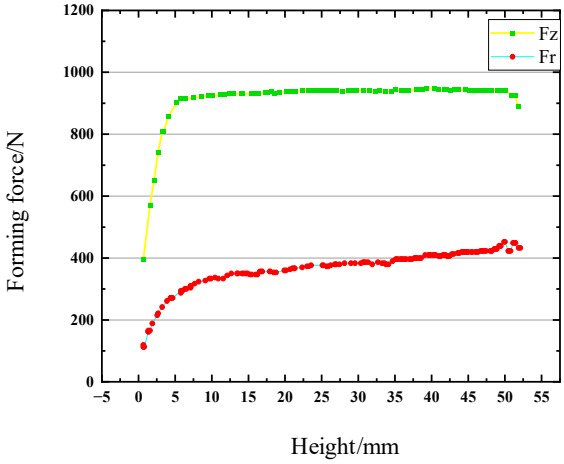

Figure 11. Radial and axial deformation forces of specimen 1.

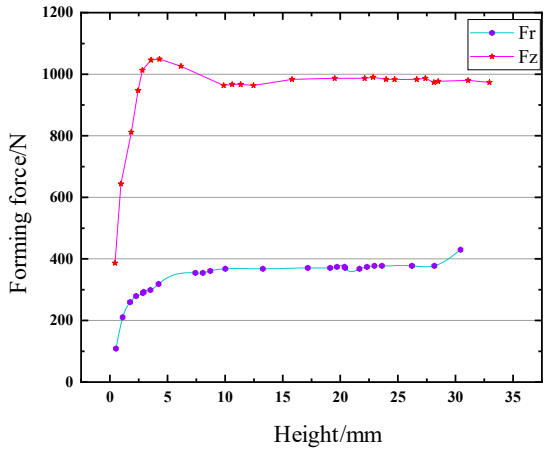

Figure 12. Radial and axial deformation forces of specimen 2.

5.2. Comparison of the Deformation Forces

Studying the forming force is the most direct starting point for the study of the incremental forming process mechanism. Many researchers have started from the mechanism to calculate the forming force after analyzing the stress and strain in the deformation area. Two main methods exist. The first consists of predicting the forming force through finite element analysis, while the second one predicts it in the forming process through empirical models obtained by experiments. Table 2 presents a comparison between the recent trends and predictions of the forming force.

Table 2. Comparison between different methods for predicting the forming force.

Methods	Results		Ref.
	Theoretical Result	Experimental Result	
Model method	897.7 N	822.0 N	[27]
	1040.0 N	1080.0 N	[32]
Finite element analysis	750.0 N	About 802.0 N	[33]
	800.0 N	About 750.0 N	[34]
Proposed method	873.6 N	932.3 N	This paper
	850.8 N	948.5 N	

It can be seen from the above analysis that when the forming enters the stable stage, the radial deformation force F_r and the axial deformation force F_Z are basically stable.

Therefore, they can be calculated as statistical measurement values. The resultant force is approximately equal to the deformation force:

$$\begin{cases} F_r = \frac{\sum_{i=1}^{n} F_{xp_i}}{n} = \frac{\sum_{i=1}^{n} F_{yp_i}}{n} \\ F_z = \frac{\sum_{i=1}^{n} F_{z_i}}{n} \\ F = \sqrt{F_r^2 + {F_z}^2} \end{cases} \tag{29}$$

The theoretical deformation force can be obtained by integrating the conditions of the two groups of forming experiments into Equations (26) and (27). Table 3 shows a comparison between the theoretically calculated value of the deformation force and its actual measured value.

Table 3. Comparison between the theoretically calculated value of the deformation force and its actual measured value.

Deformation Force	Specimen 1 (45°)			Specimen 2 (58°)		
	Calculated Value	Measured Value	Deviation	Calculated Value	Measured Value	Deviation
P_r	334.3	260.0	28.5%	412.4	336.7	22.5%
P_z	807.1	895.3	9.8%	774.1	887.1	16.1%
P	873.6	932.3	6.3%	850.8	948.8	10.3%

The findings of this study were compared with those of other studies to demonstrate the efficiency of the proposed theoretical prediction model. Veera [35] studied the impact of the forming depth, feed speed, and tool rotation speed on the forming force, and provided a model for predicting the forming force. His experimental results showed that the model's ability to predict the response value of the forming force is 95.0%. Li et al. [36] proposed a tangential force prediction and analysis model, which has an average error of 6.0% and 11.0%, respectively. This model greatly improved the prediction efficiency of the forming force. Bansal et al. [37] proposed an analytical model to predict the forming force of two different materials, reaching errors of 7.9% and 19.7%. According to the experimental results obtained in this study, the deviation of the forming resultant force is 6.3% and 10.3%, respectively, which is very close to the above experimental results, and therefore the deviation is acceptable.

6. Conclusions

This paper tackled the deformation forces of the sheet metal incremental forming process. The main conclusions are summarized as follows:

(1) The graphic approach was used to analyze the stress state of the deformation area during the forming process and the deformation of the contact region. It was also used to derive the deformation force calculation formula.

(2) The designed experiment scheme validated the accuracy of the proposed deformation force calculation method. Through experimental comparison, it was shown that the error between the theoretical analysis value and the measured value is within an acceptable range, which demonstrated the efficiency of the derived deformation force calculation method. Finally, statistical methods for measuring the radial deformation force, axial deformation force, and forming resultant force were proposed.

Author Contributions: Investigation, L.W., H.X., Q.Y., H.W. (Hao Wu) and J.K.; Formal analysis, L.W., Y.L. (Yongjie Li), S.Z., H.X., Y.L. (Yunshuang Liu), Y.Z., H.W. (Hao Wu) and Y.S.; Writing—original draft, L.W. and Y.L.; Data curation, Y.L. (Yongjie Li), S.Z., Y.L. (Yunshuang Liu), Q.Y. and Y.Z.; Visualization, S.Z., H.X., Y.L. (Yunshuang Liu) and Q.Y.; Writing—review and editing, Y.S. and J.K.; Methodology, J.K.; Funding Acquisition, H.W. (Hongyu Wei); Supervision, H.W. (Hongyu Wei). All authors have read and agreed to the published version of the manuscript.

Funding: This research was funded by the Fundamental Research Funds for the Central Universities [Grant No. NS2015055 and No.NP2020413]; the Administration of the Ministries and Commissions of the Central Government [Grant No. 011951G19061]; the National Natural Science Foundation of China [Grant No.51105202]; the State Administration of PR China and the Ministry of Education of PR China [Grant No. B16024].

Institutional Review Board Statement: Not applicable.

Informed Consent Statement: Not applicable.

Data Availability Statement: Not applicable.

Conflicts of Interest: The authors declare no conflict of interest.

References

1. Trzepieciński, T.; Oleksik, V.; Pepelnjak, T.; Najm, S.M.; Paniti, I.; Maji, K. Emerging trends in single point incremental sheet forming of lightweight metals. *Metals* **2021**, *11*, 1188. [CrossRef]
2. Farid, A.A.; Foong, S.S.; Krejcar, O.; Namazi, H. Complexity-based analysis of the effect of forming parameters on the surface finish of workpiece in single point incremental forming (SPIF). *Fractal Fract.* **2021**, *5*, 241. [CrossRef]
3. Silva, M.B.; Nielsen, P.S.; Bay, N.; Martins, P.A.F. Failure mechanisms in single-point incremental forming of metals. *Int. J. Adv. Manuf. Technol.* **2011**, *56*, 893–903. [CrossRef]
4. Shrivastava, P.; Tandon, P. Microstructure and texture based analysis of forming behavior and deformation mechanism of AA1050 sheet during single point incremental forming. *J. Mater. Process. Technol.* **2019**, *266*, 292–310. [CrossRef]
5. Nasulea, D.; Oancea, G. Achieving accuracy improvements for single-point incremental forming process using a circumferential hammering tool. *Metals* **2021**, *11*, 482. [CrossRef]
6. Lüder, S.; Lachmann, L.; Kunke, A.; Leonhardt, A.; Barthel, V.; Kräusel, V. Prediction of material failure in incremental sheet metal forming †. *Eng. Proc.* **2022**, *26*, 19.
7. Li, J.; Xie, F.; Zhao, Z.; Gono, P. Numerical simulation and fracture prediction of incremental sheet forming of metals. *J. Northeast. Univ. (Nat. Sci.)* **2019**, *40*, 488–494.
8. Tera, M.; Breaz, R.E.; Racz, S.G.; Girjob, C.E. Processing strategies for single point incremental forming—A CAM approach. *Int. J. Adv. Manuf. Technol.* **2019**, *102*, 1761–1777. [CrossRef]
9. Gandla, P.K.; Pandre, S.; Suresh, K.; Kotkunde, N. A critical analysis of formability and quality parameters for forming a dome shape using multi-stage strategies in incremental forming process. *J. Mater. Res. Technol.* **2022**, *19*, 1037–1048. [CrossRef]
10. Racz, G.S.; Oleksik, V.S.; Breaz, R.E. Incremental forming-CAE/CAM approaches and results. *IOP Conf. Ser. Mater. Sci. Eng.* **2019**, *591*, 012065. [CrossRef]
11. Alharbi, N. Experimental study on designing optimal vibration amplitude in ultrasonic assisted incremental forming of AA6061-T6. *Eng. Sci. Technol. Int. J.* **2022**, *30*, 101041. [CrossRef]
12. McAnulty, T.; Jeswiet, J.; Doolan, M. Formability in single point incremental forming: A comparative analysis of the state of the art. *CIRP J. Manuf. Sci. Technol.* **2017**, *16*, 43–54. [CrossRef]
13. Xu, P.; Li, X.; Feng, F.; Li, X.; Yang, Y. Experimental and numerical studies on two-point incremental forming of woven fabric composite sheet. *J. Manuf. Process.* **2023**, *85*, 205–215. [CrossRef]
14. Leem, D.; Liao, S.; Bhandari, S.; Wang, Z.; Ehmann, K.; Cao, J. A toolpath strategy for double-sided incremental forming of corrugated structures. *J. Mater. Process. Technol.* **2022**, *308*, 117727. [CrossRef]
15. Ullah, S.; Xu, P.; Li, X.; Li, Y.; Han, K.; Li, D. A review on part geometric precision improvement strategies in double-sided incremental forming. *Metals* **2022**, *12*, 103. [CrossRef]
16. Baharudin, B.T.H.T.; Azpen, Q.M.; Sulaima, S.; Mustapha, F. Experimental investigation of forming forces in frictional stir incremental forming of aluminum alloy AA6061-T6. *Metals* **2017**, *7*, 484. [CrossRef]
17. Jagtap, R.; Bendure, S.; Kumar, P.; Sharma, A. Experimental and simulation studies on hybrid incremental sheet forming. *Eng. Res. Express* **2022**, *4*, 025038. [CrossRef]
18. Yang, Z.; Chen, F. Mechanism of twist in incremental sheet forming of thermoplastic polymer. *Mater. Des.* **2020**, *195*, 108997. [CrossRef]
19. Benedetti, M.; Fontanari, V.; Monelli, B.; Tassan, M. Single-point incremental forming of sheet metals: Experimental study and numerical simulation. *Proc. Inst. Mech. Eng. Part B J. Eng. Manuf.* **2017**, *231*, 301–312. [CrossRef]
20. Sajjad, M.; Joy, J.A.; Jung, D.W. Finite element analysis of incremental sheet forming for metal sheet. *Key Eng. Mater.* **2018**, *783*, 148–153. [CrossRef]
21. Zhu, H.; Wang, Y.; Liu, Y.; Jung, D. The influence of sheet tilting on forming quality in single point incremental forming. *Materials* **2021**, *14*, 3907. [CrossRef] [PubMed]
22. Manish, O.; Soumen, M.; Vinay, S. Predicting the deformation force in the incremental sheet forming of AA3003. *Mater. Today Proc.* **2021**, *45*, 5069–5073.
23. Choi, H.; Lee, C. A mathematical model to predict thickness distribution and formability of incremental forming combined with stretch forming. *Robot. Comput. Integr. Manuf.* **2019**, *55*, 164–172. [CrossRef]

24. Silva, M.B.; Skjødt, M.; Martins, P.A.; Bay, N. Revisiting the fundamentals of single point incremental forming by means of membrane analysis. *Int. J. Mach. Tools Manuf.* **2008**, *48*, 73–83. [CrossRef]
25. Chang, Z.; Li, M.; Chen, J. Analytical modeling and experimental validation of the forming force in several typical incremental sheet forming processes. *Int. J. Mach. Tools Manuf.* **2019**, *140*, 62–76. [CrossRef]
26. Chang, Z.; Chen, J. Analytical modeling of fracture strain and experimental validation in incremental sheet forming. *J. Mater. Process. Technol.* **2021**, *294*, 117118. [CrossRef]
27. Aerens, R.; Eyckens, P.; Van Bael, A.; Duflou, J.R. Force prediction for single point incremental forming deduced from experimental and FEM observations. *Int. J. Adv. Manuf. Technol.* **2010**, *46*, 969–982. [CrossRef]
28. Li, Y.; Daniel, W.J.T.; Liu, Z.; Lu, H.; Meehan, P.A. Deformation mechanics and efficient force prediction in single point incremental forming. *J. Mater. Process. Technol.* **2015**, *221*, 100–111. [CrossRef]
29. Wu, J.; Xiong, D.; Li, X.; Liu, Y.; Chen, H.; Wen, L.; Dong, L.; Zheng, S.; Xu, H.; Zhang, H.; et al. Investigation on residual stress in rotational parts formed through incremental sheet forming: A novel evaluation method. *Int. J. Lightweight Mater. Manuf.* **2022**, *5*, 84–90. [CrossRef]
30. Wei, H.; Zhou, L.; Heidarshenas, B.; Ashraf, I.K.; Han, C. Investigation on the influence of springback on precision of symmetric-cone-like parts in sheet metal incremental forming process. *Int. J. Lightweight Mater. Manuf.* **2019**, *2*, 140–145. [CrossRef]
31. Ayed, L.B.; Robert, C.; Delamézière, A.; Nouari, M.; Batoz, J.L. Simplified numerical approach for incremental sheet metal forming process. *Eng. Struct.* **2014**, *62*, 75–86. [CrossRef]
32. Asghar, J.; Lingam, R.; Shibin, E.; Reddy, N.V. Tool path design for enhancement of accuracy in single-point incremental forming. *Proc. Inst. Mech. Eng. Part B J. Eng. Manuf.* **2013**, *228*, 1027–1035. [CrossRef]
33. Medina-Sanchez, G.; Garcia-Collado, A.; Carou, D.; Dorado-Vicente, R. Force prediction for incremental forming of polymer sheets. *Materials* **2018**, *11*, 1597. [CrossRef] [PubMed]
34. Moser, N.; Pritchet, D.; Ren, H.; Ehmann, K.F.; Cao, J. An efficient and general finite element model for double-sided incremental forming. *J. Manuf. Sci. Eng.* **2016**, *138*, 091007. [CrossRef]
35. Ajay, C.V. Prediction of forming force in incremental forming of Ti-6Al-4V alloy material. *Mater. Today Proc.* **2021**, *39*, 1594–1599. [CrossRef]
36. Li, Y.; Liu, Z.; Lu, H.; Daniel, W.J.T.; Liu, S.; Meehan, P.A. Efficient force prediction for incremental sheet forming and experimental validation. *Int. J. Adv. Manuf. Technol.* **2014**, *73*, 571–587. [CrossRef]
37. Bansal, A.; Lingam, R.; Yadav, S.K.; Reddy, N.V. Prediction of forming forces in single point incremental forming. *J. Manuf. Process.* **2017**, *28*, 486–493. [CrossRef]